Research Square

Preprints are preliminary reports that have not undergone peer review.
They should not be considered conclusive, used to inform clinical practice,
or referenced by the media as validated information.

Integration of a single photon source with a photonic waveguide

Aurélie Broussier
Université de Technologie de Troyes-UTT & CNRS UMR 7076
Muhammad H. Muhammad
Université de Technologie de Troyes-UTT & CNRS UMR 7076
Nancy Rahbany
Notre Dame University-Louaize
Abdelhamid Hmima
Université de Technologie de Troyes-UTT & CNRS UMR 7076
Paul Robineau
Université de Technologie de Troyes-UTT & CNRS UMR 7076
Cyrille Vezy
Université de Technologie de Troyes-UTT & CNRS UMR 7076
Régis Déturche
Université de Technologie de Troyes-UTT & CNRS UMR 7076
Antoine Kevorkian
Teem Photonics
Sylvain Blaize
Université de Technologie de Troyes-UTT & CNRS UMR 7076
Christophe Couteau
christophe.couteau@utt.fr

Université de Technologie de Troyes-UTT & CNRS UMR 7076

Article

Keywords:

Posted Date: November 7th, 2025

DOI: https://doi.org/10.21203/rs.3.rs-7718480/v1

License: This work is licensed under a Creative Commons Attribution 4.0 International License.
Read Full License

Additional Declarations: No competing interests reported.

Version of Record: A version of this preprint was published at npj Quantum Information on March 6th, 2026. See the published version at https://doi.org/10.1038/s41534-026-01209-y.

Integration of a single photon source with a photonic waveguide

Aurélie Broussier[1x], Muhammad H. Muhammad[1,2+], Nancy Rahbany[3], Abdelhamid Hmima[1], Paul Robineau[1=], Cyrille Vezy[1], Régis Déturche[1], Antoine Kevorkian[2], Sylvain Blaize[1], Christophe Couteau[1,4*]

[1]Laboratory Light, nanomaterials and nanotechnologies-L2n, Université de Technologie de Troyes-UTT & CNRS UMR 7076, 12 rue Marie Curie, 10004 Troyes Cedex, France

[2]Teem Photonics, 61 Chemin du Vieux Chêne, 38246 Meylan, France

[3]Department of Physics and Astronomy, Faculty of Natural and Applied Sciences, Notre Dame University-Louaize, Zouk Mosbeh, Lebanon

[4]EUT+ Institute of Nanomaterials and Nanotechnologies EUTINN, European University of Technology, European Union, Troyes, France

[*]Corresponding author: christophe.couteau@utt.fr
[x]Currently at FEMTO-ST Institute, Besançon, France
[+]Currently at Synopsys photonics solutions, France
[=]Currently at LASIRE, UMR 8516 CNRS-Université de Lille, Lille. France

The integration of a single photon source based on a solid-state emitter with a photonic structure remains to this day a challenging operation. It is however of prime importance to do so for quantum technologies where single photon sources constitute building blocks for many technologies and in particular for quantum photonics. In this work, we demonstrate a new way of integrating a single photon source, in our case made of a single colloidal semiconductor nanocrystal, with a photonic structure made of a glass waveguide obtained by the ion-exchange technique. Using surface functionalisation and a secondary waveguide of titanium dioxide made by electron-beam lithography, we manage to couple single photons coming from the emitter to the optical waveguide. We observe that the single photon character is preserved and demonstrates a Purcell factor of 1.2. Even though this configuration is not an optimum one, a coupling efficiency of more than 25 % is expected, compared to around 1 to 2 % we obtain for simply positioning the nanocrystal on top of the waveguide alone. The optical waveguide is then pigtailed to an optical fibre to demonstrate a first proof of principle of an integrated single photon source at room temperature.

Introduction

Optical emitters being able to provide single photons are relevant for quantum technologies in general [Cou23a,Cou23b] , for quantum photonics in particular and it is thus of paramount importance to be able to efficiently couple such quantum emitters (emitting single [Lou05,Bev02], indistinguishable [Mor20] or entangled photons [Che24]) with photonic structures such as waveguides [Bel16,Lio19], interferometers [Cre13] and optical cavities [Yan24] in order to be able to scale-up for any practical purposes. Several platforms for quantum photonics are currently explored such as epitaxial quantum dots [Pel21] where the source and the photonic parts are separated [Pon22], but also using colour centres in diamond [Nah21] or silicon carbide [Wan18] where the photonic structures are directly made within the material such as photonic crystals [Rie12]. So far, it has been evidenced difficult to bring together quantum emitters which are usually nanosized objects and 'macro' photonic-ready platforms [Pel22].

In this work, we aim to explore a new path towards bridging the "nano" to the "macro" world by connecting optically a nanosource of light with a conventional optical waveguide (WG). Our method paves the way towards scaling-up to several quantum emitters by tackling strong light-matter interfacing between photons and nanosources of light on a single optical platform. Being able to scale-up is at the heart of quantum networks [Sta22] and small-scale quantum photonics simulators [Asp12]. This differs from the usual approach of getting the greatest light extraction from nanostructures on a

substrate [Wan20]. Here we use the substrate as an active element of the device which can be seen as an optical bus.

Figure 1 is a schematic of our system where we have the photonics structure made of a semi-buried optical waveguide (using the so-called ion-exchange method [Ram88, Ter11]) made of glass and the quantum emitter (in our case a colloidal quantum dot or nanocrystal-NC) on top as the single photon emitter. In between, a secondary waveguide has been fabricated, made of a high-refractive index material, in our case titanium dioxide (TiO_2), in order to have a smooth adiabatic coupling of the nanosource to the micro-size waveguide underneath.

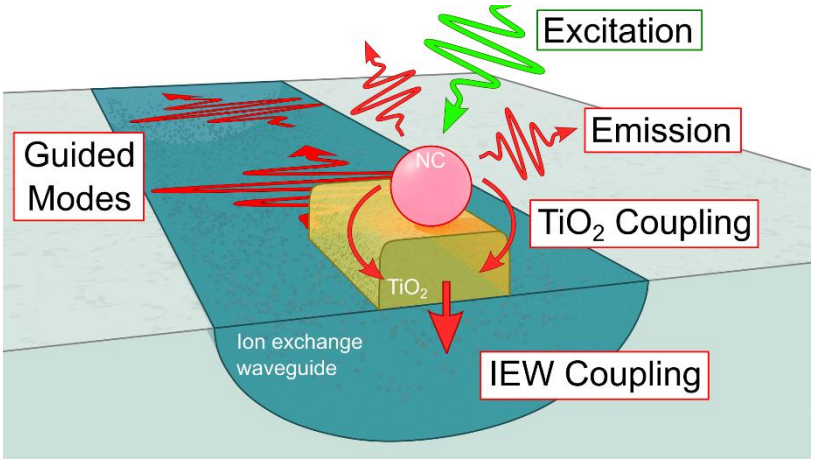


Figure 1 : Schematic of our integrated single photon source based on an ion-exchange waveguide (IEW) which allows to propagate and guide the photons emitted from a single nanocrystal (NC) thanks to the coupling with a secondary waveguide made of titanium dioxide-TiO_2.

The single photon emitter

In order to realise our integrated single photon source working at room temperature as a first proof of principle, it is necessary to use an emitter that emits single photons reliably and which does not require low temperatures. Only few emitters are relevant as single photon emitters, such as nanodiamonds [Nah21,Kha15], single molecules [Ton21] or nanocrystals [Bro04]. We use NCs as we find that more than 90 % of them are single photon emitters. The NCs are core/shell CdSe/ZnS NCs synthesized [Dab97] in-house (See Supplementary Information-SI, part S1) and are used in this work. Figure 2-a presents the typical absorption (dash orange) and emission (orange) of the NCs. We clearly see the excitonic absorption peak at 575 nm and the emission is at 610 nm (with a Full Width at Half Maximum FWHM = 25 nm). The excitation of the emission was obtained with a pulsed laser at 532 nm with a pulse rate of 5 MHz. The absorption and the fluorescence were respectively normalized to 1 for the exciton absorption peak and to the maximum of the emission. Figure 2-b presents a typical photon antibunching result of a single NC on a standard glass substrate showing a $g^{(2)}(0) = 0.14 \pm 0.05$ below 0.5 and thus ensuring we have single photon emitters. Most of the background value of the $g^{(2)}(0)$ is due to the use of a broadband filter centered at 618 nm with a rather wide FWHM of 50 nm. This brings some residual noise represented in gray in Fig 2-a. If we take into consideration this noise as well as the avalanche photodiodes (APDs) dark counts, the value would go down to $g^{(2)}(0) = 0.04 \pm 0.015$. We obtained the grey area by averaging the light detected from the laser placed on the sample where there is no NCs.

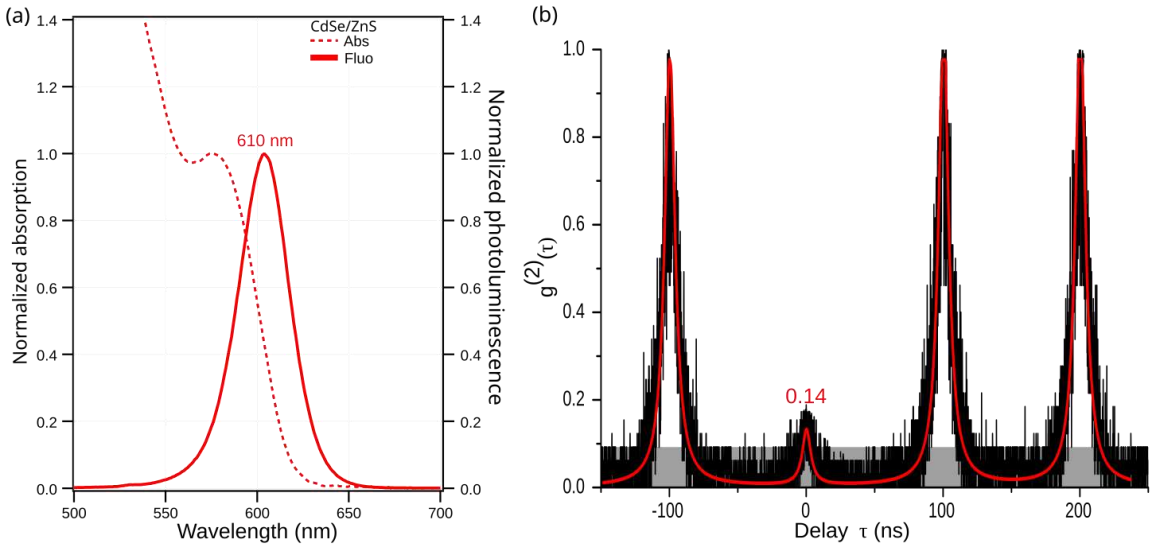


Figure 2 : (a) Normalised absorption and photoluminescence of cores/shells NCs. (b) Second order correlation function $g^{(2)}(\tau)$ for a single core/shell NC with a pulsed excitation laser at 532 nm (gray area: background light emission).

The photonic platform

For the realisation of our integrated single photon source, we use glass waveguides fabricated with the so-called ion-exchange technique [Ram88] (IEWs). In Figure 1, one can see that the coupling of the nanosources of light to the WGs is done at the surface as the waveguides are half-buried and thus allowing to interact with whatever emitter placed at their surface. IEWs are made by the exchange of sodium ions in glass with silver ions coming from a silver salt placed at the surface under heating. The exchange of ions has the consequence of changing the refractive index of the glass locally going from 1.5 or so, to 1.57 or so and thus resulting in a refractive index difference on the order of $\Delta n = 0.07$ which is enough to provide a good optical confinement of guided modes within the region of higher index due to the presence of silver ions. Using this technique, it is also possible to fabricate fully or partially buried WGs. This is one of the main advantages of using IEWs (see [Ter11] for more on such optical WGs) as opposed to laser-written waveguides [Str02] for instance which can only be within inside the bulk glass and thus cannot interact with a nanosource on top. Nevertheless, placing a single NC at the surface of an IEW is not enough to get a significant coupling of the photons emitted by the NC into the guided modes of the glass waveguides (Figure 1). Our numerical simulations show that around 1.6 % of the light emitted by an NC placed on top of the waveguide would be coupled into the IEW for a dipole (with an averaged orientation) placed at the top. It is thus important to improve the coupling of the quantum emitters to the WGs at the surface of the IEWs [Kar08]. For this, the use of a high refractive index layer in between the NC and the IEW allows a much better coupling [Bel16, Lio19]. As shown in Figure 1, we use a layer of titanium-dioxide (TiO_2) with an optical index of 2.2 (at the wavelength of 610 nm, corresponding to the emission of our NCs) [Bel16, Lio19]. Moreover, TiO_2 is a transparent material for most of the visible region where the NCs emit. In order to optimise the dimensions of the TiO_2 waveguide placed at the surface, 3D-finite difference time domain (FDTD) numerical simulations were carried out with the ion-exchange waveguide (taken with a refractive index of 1.57) in a glass substrate (taken with a refractive index of 1.5) as the one depicted in Figure 1. This structure IEW + TiO_2 has been optimised to have the best coupling efficiency. At the end, the estimated coupling efficiency from the simulation for the on-chip single photon source would be 25.9 %. Numerical simulations were also done to study the light propagation through our photonic structure, and the optimised parameters for the TiO_2 'strip' waveguide at the surface for a wavelength of 610 nm were found to be as follows: width $w = 190\ nm$, height $h = 175\ nm$ and length $L = 35\ \mu m$.

Fabrication of the photonic structure

The fabrication of the hybrid structure with the IEW and the TiO_2 strip waveguide at the surface was done in several steps. We first start from the glass waveguide which is cleaned thoroughly. In order to produce the TiO_2 strip waveguide, we use the electron-beam lithography technique. We start by depositing a layer of the well-known resin poly (methyl methacrylate) (PMMA) by spin coating it on the IEW sample. As the waveguides can be seen with an electron microscope, we center the electron beam in the middle of the guide. Our lithography system allowed us to write several guides at the same time with a spacing of 50 µm between them. The PMMA layer was then carved out via electron-beam lithography followed by 1 min development in methyl isobutyl ketone (MIBK) and 1 min in isopropanol). We then deposit the 175 nm ($h = 175\ nm$ being the optimised calculated layer) layer of TiO_2 by evaporation. After the evaporation of the TiO_2, we do not do the lift off directly in acetone. This step is performed after surface functionalisation of the TiO_2 layer with NCs. The next step is thus to place the nanocrystals (preferably single ones) on top of the TiO_2 waveguides and only there. Figure 3 presents the fabrication steps using the surface functionalisation method [Xu20]. These were necessary steps in order to realise the placement of NCs on TiO_2 layers only. For this, the sample made of the TiO_2 strip waveguide on the IEW was placed in a silane solution (3-Mercaptopropyl)-triethoxysilane (MPTES), in anhydrous ethanol + 5% H_2O, concentration between 2 to 5%) to make the "connection" between the sample surface and the quantum emitters, *i. e.* the NCs. The sample was left for 12 hours in this solution before being removed from the silane solution and rinsed with ethanol. Once the sample surface has been functionalised with silane, the sample is then placed in a toluene solution containing the NCs for 30 s which was optimized to obtain on average a single monolayer of nanocrystals with a low concentration of 10 nM so that single NCs only would be attached to the surface [Xu20]. During this step, the PMMA is removed completely and only the TiO_2 strips are left with the low concentration of NCs attached to them. At the end, 18 IEWs came out with TiO_2 strip waveguides on top after surface functionalisation of the NCs (See in SI Figure S2-1 for an optical image and Figure S2-2 for AFM images).

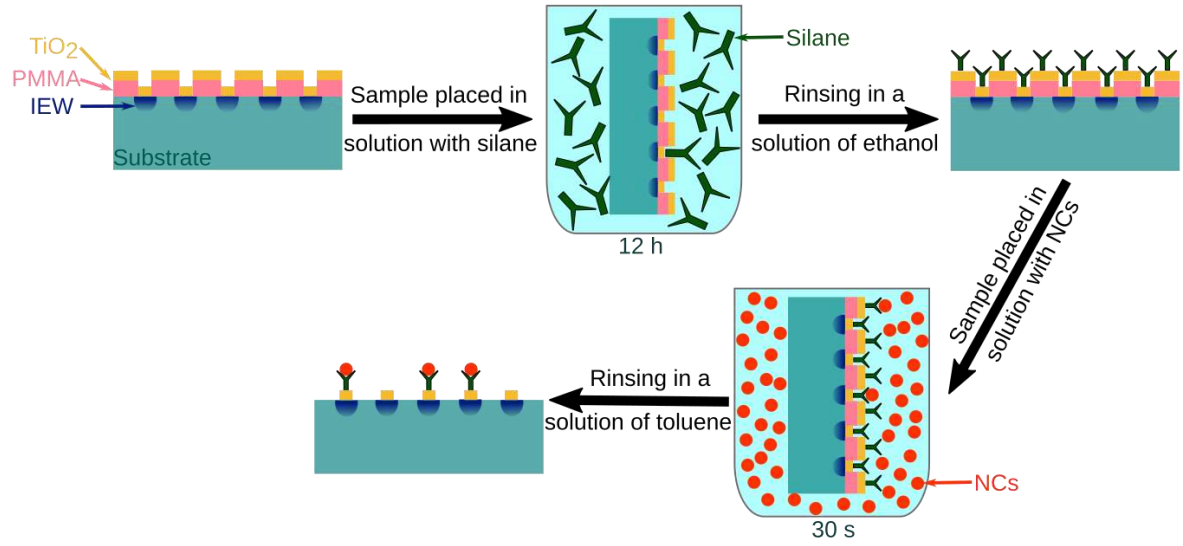


Figure 3 : Principle of surface functionalization of the NCs before lift-off of the TiO_2 structure (not to scale).

Optical characterisation

To characterise the IEW-TiO_2 structures with the nanocrystals on top, we use a home-made microphotoluminescence setup, depicted in Figure 4. A pulsed or a continuous-wave (CW) laser emitting at 532 nm is focused on the sample through a 100x objective (NA = 0.95) on the surface. The emission from the emitters is then collected via the same objective. A 650 $\pm$ 75 nm bandpass filter is

placed in front of the spectrometer to be able to cut the laser emission. For lifetime and $g^{(2)}$ autocorrelation measurements, a shorter 618 $\pm$ 25 nm bandpass filter was used. To find out if the emitter emits single photons, the light collected by the objective is sent to a 50/50 beam splitter placed before two single photon detectors (APDs) connected to a time-correlated single photon counting (TCSPC) system in order to realise the so-called Hanbury Brown and Twiss (HBT) experiment for checking whether an emitter emits single photons or not. A piezoelectric stage system (in x and y) makes it possible to realize a scan (maximum field of view of 60 µm by 60 µm) of the sample emission, thanks to the photon-counts coming from one of the detectors. This single photon detector is then connected to a home-made electronic converter which gives us a photoluminescence image of the top surface of the system such as the one in Figure 5. This piezoelectric stage system then allows us to place the excitation at the desired position once the image of the surface is obtained and when a potentially relevant NC has been identified.

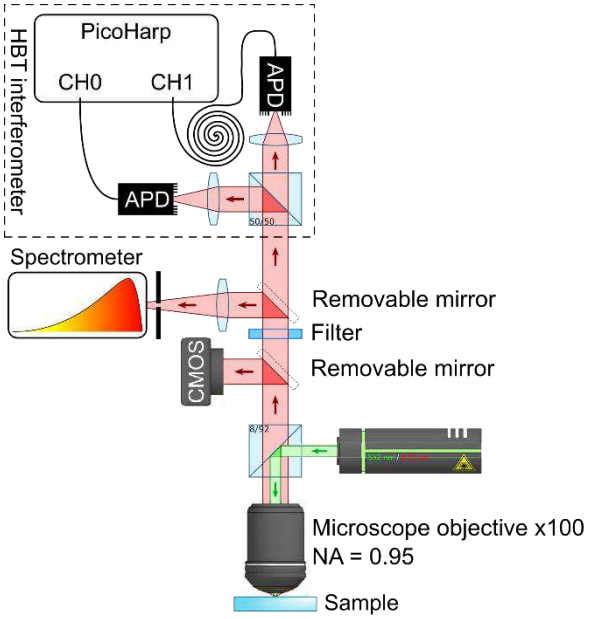


Figure 4 : Microphotoluminescence set-up used for optical characterization, with a CW or pulsed 532 nm laser as a source of excitation.

Figure 5 shows a scan of an area of 10 µm by 40 µm with a step size of 0.5 µm of the surface of the sample where one TiO_2 waveguide is found (white small rectangle). The IEW can be seen between the two white lines with a width of about 2.5 µm to be seen. More intense points can be observed (green to yellow colours), in particular, the yellow point at the position of coordinates ~ 6 µm and ~ 16 µm. The other emitting points correspond to the fluorescence of the IEW in the range of 575 to 725 nm (which can thus be seen, through our bandpass filter) by the excitation at 532 nm due mostly to the silver ions contained in the ion-exchange WG [Wei18].

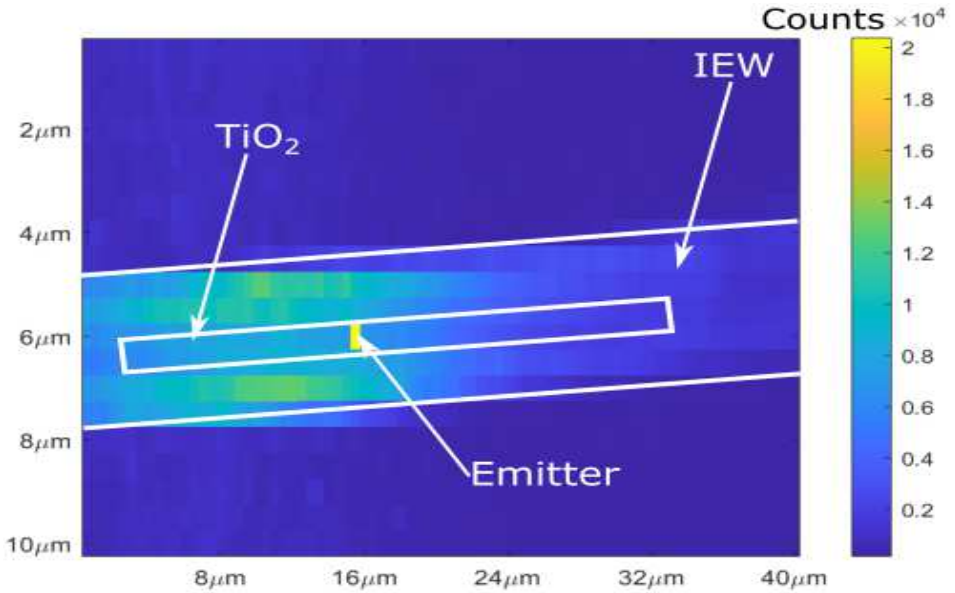


Figure 5 : A 10 µm by 40 µm photoluminescence scan image of a TiO_2 structure on an ion-exchange waveguide with a single NC emitting. Excitation is done at 532 nm with a bandpass filter 650 ± 75 nm.

On this waveguide, the 532 nm laser spot was then placed at the supposedly NC point level of the image from Figure 5 thanks to the piezoelectric stage system. The black spectrum in Figure 6-a represents the emission from this point (the bright yellow point in Figure 5) via the collection from the top microscope objective, excited by the 532 nm CW laser. On the black spectrum, an emission peak at 610 nm (FWHM ≈ 28 nm) is present. This peak corresponds to the emission of the NCs that we presented previously (Figure 2-a). On this spectrum, in addition to the NC emission we observe a weaker and broader peak centered around 680 nm. This broad peak corresponds to fluorescence coming from the IEW-TiO_2 structure. Indeed, when we place the laser directly on the TiO_2 structure on the guide, the blue spectrum of Fig. 6-a is obtained by the top detection from the objective. In fact, the waveguide fluorescence shows two broad peaks at 620 and 680 nm respectively (See S3 and Figure S3-1 in SI). These two peaks are attributed to the insertion of silver ions in the glass waveguide to form the IEW [Wei98] (see S3 in SI). The photoluminescence of the strip (white small rectangle) of TiO_2 directly on glass presented an emission peak at 675 nm [Has10] (see the pink curve in Figure S3-1b). Thus, the peak at 620 nm is attributed to the silver ion luminescence alone while the peak at 680 nm has the contribution of silver ions and defects from the TiO_2 layer. This sample containing potentially a single NC on the photonic structure was then fibre-pigtailed (see inset of Figure 6-a). The red spectrum from Figure 6-a represents the emission spectrum coming out from the fibre of the photonic platform with a top excitation. We can observe that the background fluorescence from the silver ions in the IEW and from the TiO_2 layer is mostly filtered out and is not guided by the IEW. The NC emitter was then tested with our HBT interferometer to find out if it is truly a single photon emitter. The $g^{(2)}$ result under a pulsed laser excitation at 532 nm is shown in Figure 6-b. The obtained value of $g^{(2)}(0) = 0.24 \pm 0.1$ for the emission peak at zero delay is clear evidence that we have a single photon source from the NC emission. Once again, the non-ideal $g^{(2)}(0)$ result is due to the parasitic luminescence from the IEW and the TiO_2 strip as just discussed. After removal of the background light (grey area in Figure 6-b), we can obtain a value of $g^{(2)}(0) = 0.14$, which clearly proves the emission of a single photon. We studied other nanocrystals with more waveguides with a fibre output giving a $g^{(2)}(0)$ corresponding to a single photon emitter (see S4 in Supplementary Information).

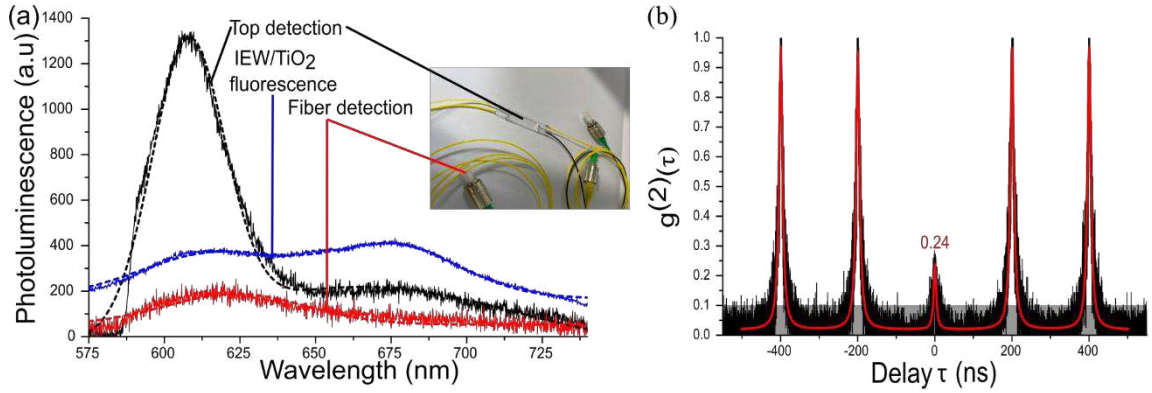


Figure 6 : (a) Photoluminescence from the NC from identified in Figure 6: in black the spectrum is measured on top of the IEW-TiO_2, structure, in blue is the residual fluorescence coming from the IEW-TiO_2 structure and in red is the fluorescence at the fibre end with an excitation laser at 532 nm, (b) second order correlation function for the single NC on top of the IEW-TiO_2 structure excited from the top with a pulsed excitation and collected from the fibre connected to the waveguide (in gray: background level due to broad filtering).

To get an idea of the coupling between the single NC and the waveguide via the TiO_2 photonic structure, measurements of the lifetime of this NC were carried out. Figure 7 represents the lifetime measurement under a 532 nm pulsed laser excitation at a 5 MHz repetition rate, respectively for NCs on a glass substrate alone (in black) and of a single NC on the photonic hybrid structure (in red) (see more in section S3 in SI). In the presence of the TiO_2 structure on the IEW, the lifetime of the NC decreases compared to its lifetime on the substrate reference. To validate the fluorescence decay rate, the data were fitted using a bi-exponential model according to the equation $I(t) = I_0 + A_1 e^{\frac{-t}{\tau_1}} + A_2 e^{\frac{-t}{\tau_2}}$. Using this fitted model, excited state lifetimes of $\tau_1 = 3.39\ ns$ and of $\tau_2 = 20.09\ ns$ for NCs on the glass substrate alone and excited state lifetimes of $\tau_1 = 3.05\ ns$ and of $\tau_2 = 16.53\ ns$ for a single NC on the photonic IEW/TiO_2 structure were found.

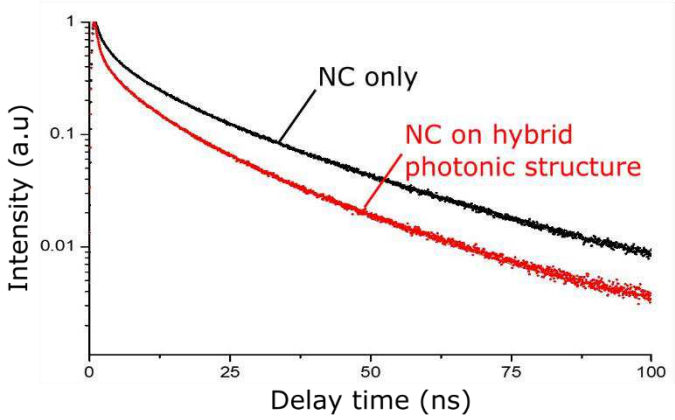


Figure 7 : In black is the average lifetime measurement of 10 single NCs on a glass substrate alone and in red is the average lifetime measurement of 3 single NCs on the IEW/TiO_2 photonic structure.

The lifetime measurement represents the NC decay rate of the excited state. It thus includes the radiative Γ_{rad} and non-radiative Γ_{nr} decay rates $\Gamma = \Gamma_{rad} + \Gamma_{nr}$. From the lifetimes obtained on the different structures, the Purcell factor can be calculated as follows $P_f = \frac{\Gamma}{\Gamma_0} = \frac{\tau_0}{\tau}$, with τ_0 and τ representing respectively the averaged NC lifetime on a glass substrate and on the IEW/TiO_2 structure in our case. In the case of Figure 7, a Purcell factor of 1.19 ± 0.01 was deduced for a single NC whereas simulations provided a Purcell Factor of 1.45. The discrepancy can come from a specific orientation of the dipole (whereas simulations are taken with an average orientation) or from a difference in the

experimental optical coupling with structure, itself with some imperfections. This is however consistent with results obtained previously with a similar structure and an ensemble of NCs [Bel16, Lio19]. The Purcell factor of a single NC on the waveguide alone is 1.08 whereas simulations predict a value of 1.11. Thus, as expected, by adding a high index structure of TiO_2 onto the waveguide, it is possible to increase the Purcell factor and to increase the coupling efficiency in the guide.

Conclusion and perspectives

In this paper, we have presented a fibered single photon source based on a hybrid photonic structure. The use of an ion-exchange glass waveguide makes it possible to have a fibered source emitting single photon at room temperature. The addition of the high index structure of TiO_2 to the emitter allows better coupling into the waveguide or around 25 %. The use of a plasmonic antenna will increase even more so this coupling with first simulation results showing coupling over 95 % in some cases [Luo15]. Moreover, this work was using colloidal semiconductor quantum dots, but it paves the way towards more relevant emitters for quantum technologies such as colour centre in nanodiamonds where first results of positioning such nanoparticles using similar techniques as already been demonstrated [Iss21].

Acknowledgements and funding statement

The authors would like to thank the Graduate School (École Universitaire de Recherche) “NANO-PHOT”, contract ANR-18-EURE-0013, they acknowledge the use of the nano’mat platform from the CNRS Renatech network and funding from the FEDER, the Grand Est Region and the Aube Department. This work received support from French National Agency for Research-ANR of the OQuLuS project under the France 2030 initiative, contract ANR-23-PETQ-0013. The authors thank CNRS-Innovation and the SATT SAYENS for funding A. B. via the projects InteQ and InteQ2.

Author contributions

A. B. contributed to the fabrication and characterisation work and contributed significantly to the writing of the article, M. H. M. contributed to the characterisation and simulation work, N. R. contributed to the simulation work, A. H. contributed to the fabrication work, P. R. & C. V. contributed to the synthesis work, R. D. contributed to the data acquistion of the work, A. K. contributed to the discussions, S. B. contributed to the discussions, C. C. designed and supervised the work & contributed significantly to the writing of the article as well as the discussions. All authors reviewed the article.

Competing interests

The authors declare no competing interests.

Bibliography:

[Cou23a] Couteau, C.; Barz, S.; Durt, T.; Gerrits, T.; Huwer, J.; Prevedel, R.; Rarity, J.; Shields, A.; Weihs, G. Applications of Single Photons to Quantum Communication and Computing. Nat Rev Phys 2023, 5 (6), 326–338. https://doi.org/10.1038/s42254-023-00583-2.
[Cou23b] Couteau, C.; Barz, S.; Durt, T.; Gerrits, T.; Huwer, J.; Prevedel, R.; Rarity, J.; Shields, A.; Weihs, G. Applications of Single Photons in Quantum Metrology, Biology and the Foundations of Quantum Physics. Nat Rev Phys 2023, 5 (6), 354–363. https://doi.org/10.1038/s42254-023-00589-w.
[Lou05] Lounis, B.; Orrit, M. Single-Photon Sources. *Rep. Prog. Phys.* **2005**, *68* (5), 1129–1179. https://doi.org/10.1088/0034-4885/68/5/R04.
[Bev02] Beveratos, A.; Kühn, S.; Brouri, R.; Gacoin, T.; Poizat, J.-P.; Grangier, P. Room Temperature Stable Single-Photon Source. *Eur. Phys. J. D* **2002**, *18* (2), 191–196. https://doi.org/10.1140/epjd/e20020023.
[Mor20] Morioka, N.; Babin, C.; Nagy, R.; Gediz, I.; Hesselmeier, E.; Liu, D.; Joliffe, M.; Niethammer, M.; Dasari, D.; Vorobyov, V.; Kolesov, R.; Stöhr, R.; Ul-Hassan, J.; Son, N. T.; Ohshima, T.; Udvarhelyi, P.; Thiering, G.; Gali, A.; Wrachtrup, J.; Kaiser, F. Spin-Controlled Generation of Indistinguishable and Distinguishable Photons from Silicon Vacancy Centres in Silicon Carbide. *Nat Commun* **2020**, *11* (1), 2516. https://doi.org/10.1038/s41467-020-16330-5.
[Che24] Chen, C., Yan, JY., Babin, HG. et al. Wavelength-tunable high-fidelity entangled photon sources enabled by dual Stark effects. Nat Commun 15, 5792 (2024). https://doi.org/10.1038/s41467-024-50062-0
[Bel16] Beltran Madrigal, J.; Tellez-Limon, R.; Gardillou, F.; Barbier, D.; Geng, W.; Couteau, C.; Salas-Montiel, R.; Blaize, S. Hybrid Integrated Optical Waveguides in Glass for Enhanced Visible Photoluminescence of Nanoemitters. *Applied Optics* **2016**, *55* (36), 10263. https://doi.org/10.1364/AO.55.010263.
[Lio19] Integration of Nanoemitters onto Photonic Structures by Guided Evanescent-Wave Nano-Photopolymerization. Giuseppe Emanuele Lio, Josslyn Beltran Madrigal, Xiaolun Xu, Ying Peng, Stefano Pierini, Christophe Couteau, Safi Jradi, Renaud Bachelot, Roberto Caputo, Sylvain Blaize. J. Phys. Chem. C 2019, 123, 14669−14676.
[Cre13] Crespi, A.; Osellame, R.; Ramponi, R.; Brod, D. J.; Galvão, E. F.; Spagnolo, N.; Vitelli, C.; Maiorino, E.; Mataloni, P.; Sciarrino, F. Integrated Multimode Interferometers with Arbitrary Designs for Photonic Boson Sampling. *Nature Photon* **2013**, *7* (7), 545–549. https://doi.org/10.1038/nphoton.2013.112.
[Yan24] Yang, J., Chen, Y., Rao, Z. *et al.* Tunable quantum dots in monolithic Fabry-Perot microcavities for high-performance single-photon sources. *Light Sci Appl* **13**, 33 (2024). https://doi.org/10.1038/s41377-024-01384-7
[Pel21] Semiconductor quantum dots: Technological progress and future challenges. F. Pelayo García de Arquer, Dmitri V. Talapin, Victor I. Klimov, Yasuhiko Arakawa, Manfred Bayer, and Edward H. Sargent. Science 373, 640 (2021). DOI: 10.1126/science.aaz8541
[Pon22] Pont, M.; Albiero, R.; Thomas, S. E.; Spagnolo, N.; Ceccarelli, F.; Corrielli, G.; Brieussel, A.; Somaschi, N.; Huet, H.; Harouri, A.; Lemaître, A.; Sagnes, I.; Belabas, N.; Sciarrino, F.; Osellame, R.; Senellart, P.; Crespi, A. Quantifying N-Photon Indistinguishability with a Cyclic Integrated Interferometer. *Phys. Rev. X* **2022**, *12* (3), 031033. https://doi.org/10.1103/PhysRevX.12.031033.
[Nah21] Nahra, M.; Alshamaa, D.; Deturche, R.; Davydov, V.; Kulikova, L.; Agafonov, V.; Couteau, C. Single Germanium Vacancy Centers in Nanodiamonds with Bulk-like Spectral Stability. *AVS Quantum Sci.* **2021**, *3* (1), 012001. https://doi.org/10.1116/5.0035937.
[Wan18] Wang, J.; Zhou, Y.; Wang, Z.; Rasmita, A.; Yang, J.; Li, X.; von Bardeleben, H. J.; Gao, W. Bright Room Temperature Single Photon Source at Telecom Range in Cubic Silicon Carbide. *Nat*

Commun **2018**, *9* (1), 4106. https://doi.org/10.1038/s41467-018-06605-3.
[Rie12] Riedrich-Möller, J., Kipfstuhl, L., Hepp, C. *et al.* One- and two-dimensional photonic crystal microcavities in single crystal diamond. *Nature Nanotech* **7**, 69–74 (2012). https://doi.org/10.1038/nnano.2011.190
[Pel22] Pelucchi, E.; Fagas, G.; Aharonovich, I.; Englund, D.; Figueroa, E.; Gong, Q.; Hannes, H.; Liu, J.; Lu, C.-Y.; Matsuda, N.; Pan, J.-W.; Schreck, F.; Sciarrino, F.; Silberhorn, C.; Wang, J.; Jöns, K. D. The Potential and Global Outlook of Integrated Photonics for Quantum Technologies. *Nat Rev Phys* **2022**, *4* (3), 194–208. https://doi.org/10.1038/s42254-021-00398-z.
[Sta22] Stas, P.-J.; Huan, Y. Q.; Machielse, B.; Knall, E. N.; Suleymanzade, A.; Pingault, B.; Sutula, M.; Ding, S. W.; Knaut, C. M.; Assumpcao, D. R.; Wei, Y.-C.; Bhaskar, M. K.; Riedinger, R.; Sukachev, D. D.; Park, H.; Lončar, M.; Levonian, D. S.; Lukin, M. D. Robust Multi-Qubit Quantum Network Node with Integrated Error Detection. *Science* **2022**, *378* (6619), 557–560. https://doi.org/10.1126/science.add9771.
[Asp12] Aspuru-Guzik, A., Walther, P. Photonic quantum simulators. *Nature Phys* **8**, 285–291 (2012). https://doi.org/10.1038/nphys2253
[Wan20] Wang, J.; Sciarrino, F.; Laing, A.; Thompson, M. G. Integrated Photonic Quantum Technologies. *Nat. Photonics* **2020**, *14* (5), 273–284. https://doi.org/10.1038/s41566-019-0532-1.
[Ram88] Ramaswamy, R. V.; Srivastava, R. Ion-Exchanged Glass Waveguides: A Review. *Journal of Lightwave Technology* **1988**, *6* (6), 984–1000. https://doi.org/10.1109/50.4090.
[Kha15] Khalid, A.; Chung, K.; Rajasekharan, R.; Lau, D. W. M.; Karle, T. J.; Gibson, B. C.; Tomljenovic-Hanic, S. Lifetime Reduction and Enhanced Emission of Single Photon Color Centers in Nanodiamond via Surrounding Refractive Index Modification. *Sci Rep* **2015**, *5* (1), 11179. https://doi.org/10.1038/srep11179.
[Ton21] Toninelli, C.; Gerhardt, I.; Clark, A. S.; Reserbat-Plantey, A.; Götzinger, S.; Ristanović, Z.; Colautti, M.; Lombardi, P.; Major, K. D.; Deperasińska, I.; Pernice, W. H.; Koppens, F. H. L.; Kozankiewicz, B.; Gourdon, A.; Sandoghdar, V.; Orrit, M. Single Organic Molecules for Photonic Quantum Technologies. *Nat. Mater.* **2021**, *20* (12), 1615–1628. https://doi.org/10.1038/s41563-021-00987-4.
[Bro04] Brokmann, X.; Messin, G.; Desbiolles, P.; Giacobino, E.; Dahan, M.; Hermier, J. P. Colloidal CdSe/ZnS Quantum Dots as Single-Photon Sources. *New J. Phys.* **2004**, *6*, 99–99. https://doi.org/10.1088/1367-2630/6/1/099.
[Dab97] Dabbousi, B. O.; Rodriguez-Viejo, J.; Mikulec, F. V.; Heine, J. R.; Mattoussi, H.; Ober, R.; Jensen, K. F.; Bawendi, M. G. (CdSe)ZnS Core−Shell Quantum Dots: Synthesis and Characterization of a Size Series of Highly Luminescent Nanocrystallites. *J. Phys. Chem. B* **1997**, *101* (46), 9463–9475. https://doi.org/10.1021/jp971091y.
[Ter11] Ari Tervonen, Seppo K. Honkanen, and Brian R. West "Ion-exchanged glass waveguide technology: a review," Optical Engineering 50(7), 071107 (1 July 2011). https://doi.org/10.1117/1.3559213
[Str02] Streltsov, A. M.; Borrelli, N. F. Study of Femtosecond-Laser-Written Waveguides in Glasses. *J. Opt. Soc. Am. B, JOSAB* **2002**, *19* (10), 2496–2504. https://doi.org/10.1364/JOSAB.19.002496.
[Kar08] Karasiński, P.; Rogoziński, R. Characterization and Sensor Properties of Sol–Gel SiO2:TiO2 Film/Ion-Exchange Glass Optical Waveguides. *Optics Communications* **2008**, *281* (9), 2472–2480. https://doi.org/10.1016/j.optcom.2007.12.068.
[Wei18] Wei, H.; Pan, D.; Zhang, S.; Li, Z.; Li, Q.; Liu, N.; Wang, W.; Xu, H. Plasmon Waveguiding in Nanowires. *Chemical Reviews* **2018**, *118* (6), 2882–2926. https://doi.org/10.1021/acs.chemrev.7b00441.
[Xu20] Xu, X.; Broussier, A.; Ritacco, T.; Nahra, M.; Geoffray, F.; Issa, A.; Jradi, S.; Bachelot, R.; Bachelot, R.; Bachelot, R.; Couteau, C.; Couteau, C.; Blaize, S.; Blaize, S. Towards the Integration of

Nanoemitters by Direct Laser Writing on Optical Glass Waveguides. *Photon. Res., PRJ* **2020**, *8* (9), 1541–1550. https://doi.org/10.1364/PRJ.392706.
[Wei98] Weisser, M.; Thoma, F.; Menges, B.; Langbein, U.; Mittler-Neher, S. Fluorescence in Ion Exchanged BK7 Glass Slab Waveguides and Its Use for Scattering Free Loss Measurements. *Optics Communications* **1998**, *153* (1), 27–31. https://doi.org/10.1016/S0030-4018(98)00222-3.
[Han10] Hassanzadeh, A.; Nitsche, M.; Armstrong, S.; Nabavi, N.; Harrison, R.; Dixon, S. J.; Langbein, U.; Mittler, S. Optical Waveguides Formed by Silver Ion Exchange in Schott SG11 Glass for Waveguide Evanescent Field Fluorescence Microscopy: Evanescent Images of HEK293 Cells. *J. Biomed. Opt.* **2010**, *15* (3), 036018. https://doi.org/10.1117/1.3443796.
[Luo15] On-Chip Hybrid Photonic–Plasmonic Light Concentrator for Nanofocusing in an Integrated Silicon Photonics Platform. Ye Luo, Maysamreza Chamanzar, Aniello Apuzzo, Rafael Salas-Montiel, Kim Ngoc Nguyen, Sylvain Blaize, Ali Adibi. Nano Lett. 2015, 15, 849−856.
[Iss21] One Strategy for Nanoparticle Assembly onto 1D, 2D, and 3D Polymer Micro and Nanostructures. Ali Issa, Irene Izquierdo, Melissa Merheb, Dandan Ge, Aurélie Broussier, Nawres Ghabri, Sylvie Marguet, Christophe Couteau, Renaud Bachelot, Safi Jradi. ACS Appl. Mater. Interfaces 2021, 13, 41846−41856.

Supplementary Files

This is a list of supplementary files associated with this preprint. Click to download.

- articleIEWQDSIv14bis.docx